Demagnetization of thick section steels for electron beam welding

Colin Ribton

High power electron beam welding can be applied to structures such as pressure vessels with wall thicknesses of up to 200 mm. Such applications often make use of steels that exhibit ferro-magnetic properties. If the work pieces acquire a magnetic field, on assembly it has been found that reasonably strong external fields can be measured. Such fields do not need to be greater than 0.2 mT to cause an electron beam to be deflected, and such deflection can lead to missed joint defects at the cap or root of the weld. Correction of these weld defects in thick sections is costly.

This paper examines in detail the magnetic behavior of a steel frequently selected for nuclear plant – A508 grade 3. It has frequently been observed that this grade of steel can be more problematic to demagnetize, and beam deflection has been observed if no counter measures are taken. Special equipment has been designed to carry out the demagnetization of large segments, 200 mm thick and some 900 mm in length. A new approach has been taken to monitoring the magnetic field during the demagnetization cycle, which allows the effectiveness of the process to be assessed. Within this paper, magnetic modelling results, the demagnetization equipment, instrumentation and results are presented.

Keywords – Demagnetization, Electron beam, Steel, Thick section.

Introduction

There is increasing interest internationally in developing a radically different approach to the deployment of nuclear power for power generation, which would be used alongside conventional nuclear, wind, solar, hydropower and other low-carbon energy sources to support a secure and affordable energy supply. This approach will be characterised by the use of small modular reactors to provide electricity and process heat.

Modern nuclear reactors used in conventional power stations typically provide 1600 MW of electricity. In contrast, an SMR is defined as a reactor providing less than 300 MW of electricity, although this is not a firm limit. Its design draws upon the experience of building and operating marine power units over the past 65 years. It will be produced in modular form (e.g. 100 each year), giving an economy of scale, and be transportable so it can be freighted from the factory to the site. It also will require much less site preparation – all of which reduces the capital risk and cost for the installation. The approach will allow incremental expansion of power production capability on any given site, or the installation of replacement plant on brown-field sites, such as decommissioned fossil fuel power stations.

Although there are some 30 different designs of SMR under development, most of them include a pressure vessel to contain the steam generation plant. Production of pressure vessels requires welding of thick section steel of up to 200 mm. Although this can be addressed using arc welding techniques, electron beam welding offers much higher productivity.

Within the overall project, TWI have investigated the use of electron beam welding for construction of 200 mm thick pressure vessels in A508 grade 3 material for small modular reactors. One of the challenges of thick section electron beam welding in ferro-magnetic steels arises due to magnetic fields causing beam deflection and weld defects. We needed to be sure that test pieces and the demonstrator parts can be demagnetized as fields of 0.1 mT can cause significant electron beam deflection leading to weld defects.

Our experience with electron beam welding of A508 grade 3 has been that the material will have significant external magnetic fields even if not exposed to magnetic fields from lifting gear or other equipment. These presumably are induced by the earth’s field and mechanical vibration. Consequently, it is necessary to develop an effective demagnetisation strategy as part of the welding procedure for SMR pressure vessels.

This report covers the investigative work carried out on the demagnetization of A508 grade 3 material. This includes:

- Modelling of TWI's demagnetization yoke for test blocks;
- Measurement during demagnetization cycling of test blocks;
- Modelling to determine requirements for demagnetization of demonstrator parts.

The work has used a combination of magnetic simulation finite element analysis software and instrumentation during practical trials to gain an insight into the magnetic state of test blocks. Data from previous work (in particular the measured B/H characteristic of A508 grade 3) has been used in the modelling.

Objectives

The objectives of this work were:

- To successfully demagnetize test blocks such that there was no magnetic interference in the welding work;
- To understand demagnetization techniques and why they are successful;
- To recommend the optimum demagnetization methods and equipment for the large demonstrator parts.

Work carried out

Modelling of TWI's demagnetisation yoke for test blocks

TWI have a large soft iron yoke that can be used to boost the applied H field during demagnetization of test pieces. This is shown in Fig. 1.

Fig. 1. TWI's demagnetization equipment.

A model of the yoke and work piece was constructed for finite element analysis. Symmetry allows half of the yoke to be modelled and it was modelled in two dimensions with *XY* symmetry, see Fig. 2. The boundary conditions were that on the symmetry boundary the flux lines are forced to be normal to the boundary, and on the other boundaries the flux lines were forced to be tangential. The figure shows the initial model with linear material properties and a coarse mesh.

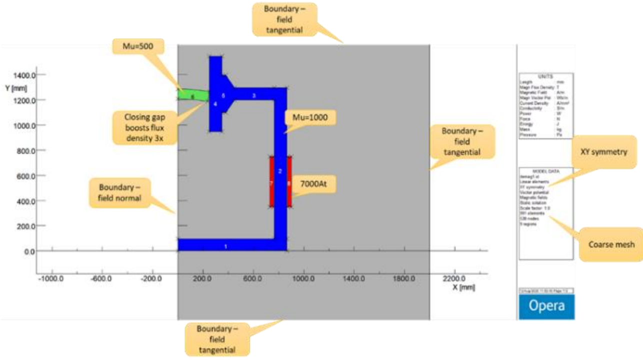

Fig. 2. Initial model of the demagnetizer yoke.

The mesh was refined, see Fig. 3, and the *B* field achieved in the test block was measured along the axis of symmetry (the *Y* axis), see Fig. 4. The wedge pieces were added in the model and in real life, as a small air gap represents a high magnetic reluctance, and reduces the *B* field achieved for the same coil excitation.

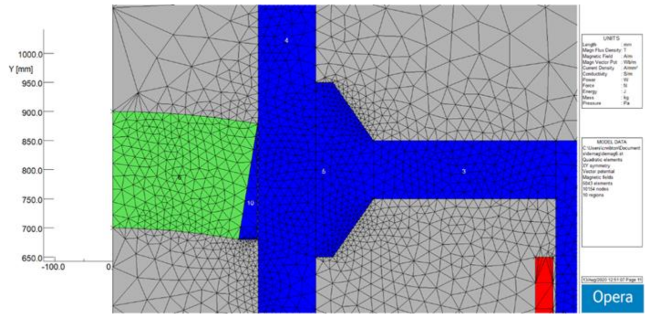

Fig. 3. Refined mesh in the yoke and test block.

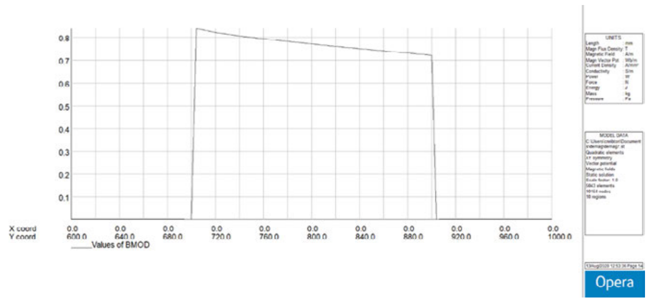

Fig. 4. B field measured through the test block on the Y axis.

Data previously collected on A508 grade 3 was used in the model. The initial magnetization curve for A508 grade 3 is shown in Fig. 5.

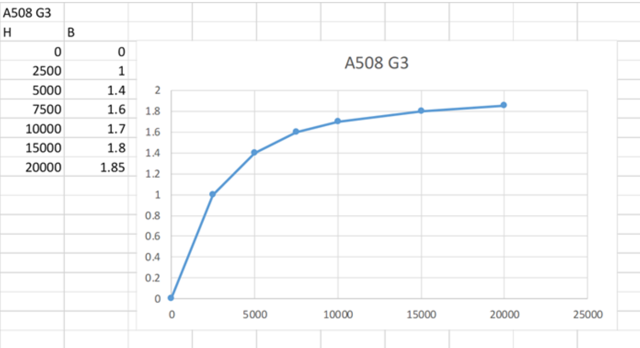

Fig. 5. Initial magnetization curve of A508 grade 3.

With non-linear materials (i.e. with a B/H curve entered for the test block and the yoke materials) it is possible to look at the magnetic saturation achieved, see Fig. 6, for a coil excitation of 6.600 At (66 turns and 100 A maximum) for this half of the model. Magnetic saturation is achieved when the relative permeability of the material approaches a value of one. It is expected that magnetic saturation will be required to some degree in order to demagnetize successfully.

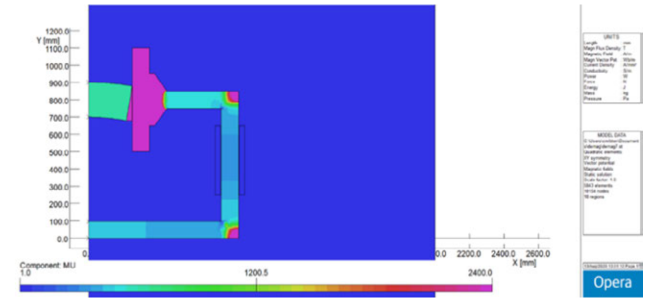

Fig.6. Plot showing the magnetic permeability in the yoke and test block.

As the yoke arms are thinner than the test block, the flux density in the test block is correspondingly lower, reducing the level of material saturation (Fig. 6). However, on the actual yoke, the cross-sectional are of the yoke arms and the test block are the same – the yoke is 600 mm x 100 mm and the test blocks are 200 mm x 300 mm. If we adjust the two dimensional model to account for the same cross-sectional area, i.e. by making the yoke arms the same thickness as the test block, we obtain a much higher magnetic field in the test block, see Fig. 7.

This higher field translates into a convincing saturation of the test block, see Fig. 8, where the test block permeability is close to one.

This saturation is achieved as the B field measured in the block on the Y axis of the model is 1.5T.

As a consequence of this modelling of the demagnetizer yoke and test blocks we could be confident that a reasonable level of saturation of the test blocks would be possible.

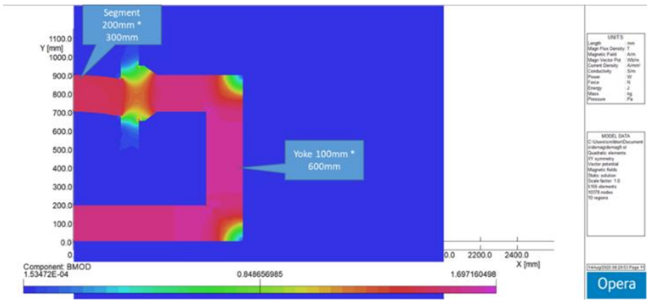

Fig. 7. The magnetic field plot for the yoke and test block when the yoke arms have been compensated for having the same cross-sectional area as the test block.

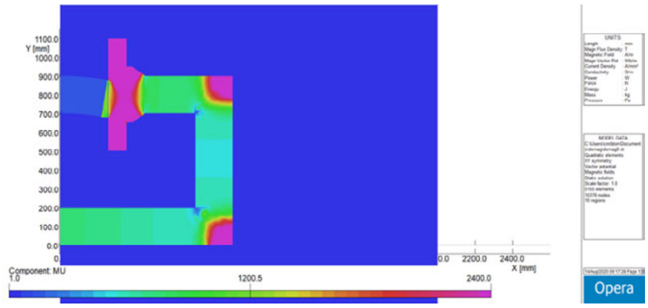

Fig. 8. Plot of the magnetic permeability with corrected yoke arm cross-sectional area.

Measurement during demagnetization cycling of test blocks

It was found that measuring the external field around a test block was not a good indicator of whether a block was completely demagnetized. Often if it was assembled with another block a large magnetic field could be measured in the gap between them. Consequently, instrumentation and techniques were developed to measure the B field in the blocks using search coils during demagnetization.

Search coils were constructed with multi-pole connectors, which allowed the coils to be rapidly put on the work piece and the yoke, see Fig. 9.

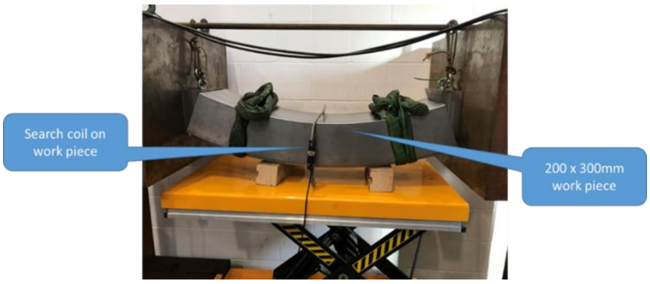

Fig. 9. Search coil connected around the work piece segment.

The configuration for the demagnetization cycling is shown schematically in Fig. 10.

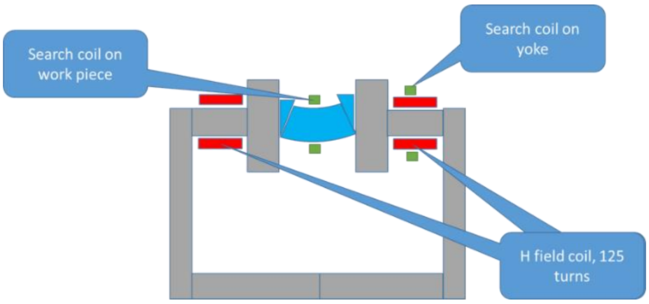

Fig. 10. Schematic of coil arrangements on the demagnetizer.

A typical demagnetization cycle used initially a 100A sine wave with a period of two minutes. After this the current for each cycle decreased linearly to zero over 25 cycles of the same period. The *H* field was determined by measuring the current through the *H* field coil using a current clamp. Knowing also the length of the magnetic path (i.e. the length around the yoke and work piece) and the number of coil turns, the H field was then calculated:

$$H = A.N/length$$

The *B* field in the work piece or yoke was then found by measuring the voltage in the search coil. Knowing the number of turns in the search coil and its area allowed the *B* field to be calculated as:

$$B = \int (Vs/(Ns.As))dt$$

It was found necessary to correct for integrator drift as small offsets accumulated over the long demagnetization cycle. The signals were collected on a data logger (picologger ADC20) and processed with a Python script, see Fig. 11. It was noted that there was sometimes a difference between the *B* field in the yoke and that in the work piece. This could be an indication of some initial magnetization and can be seen to reduce to zero in the first few cycles.

When there was significant magnetization of the test piece there was clear polarization of the B field, despite the H field being symmetric, see Fig. 12.

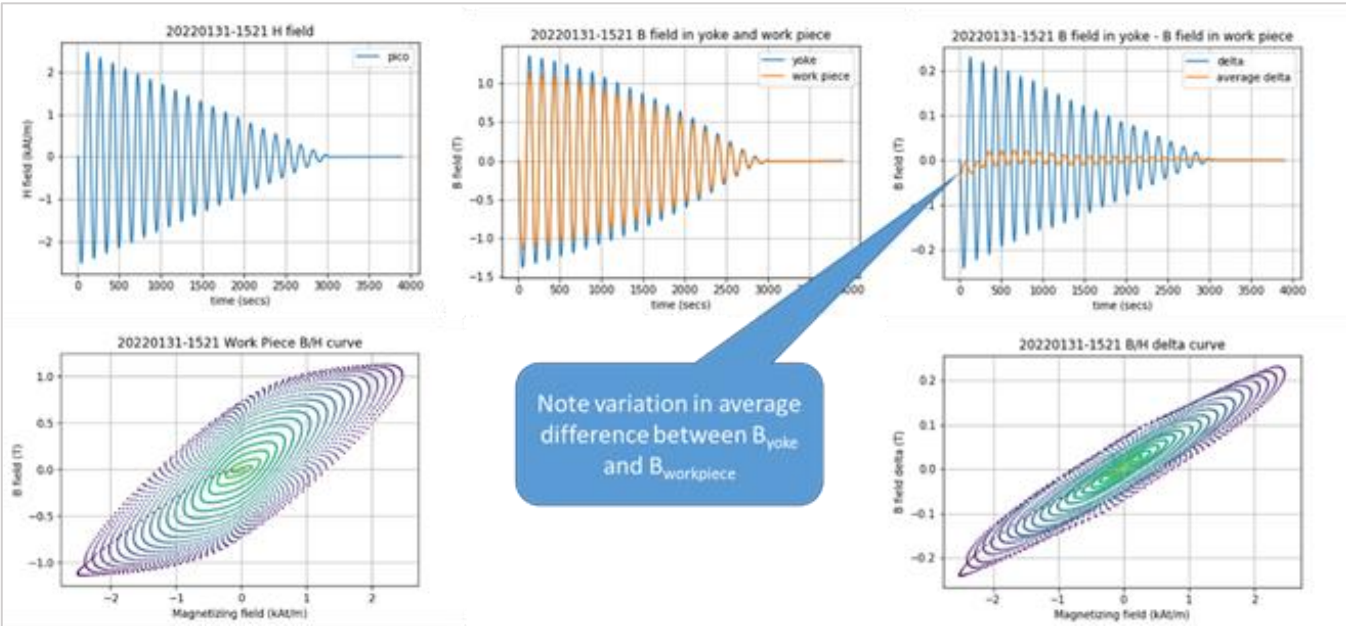

Fig. 11. Typical collected data from a successful demagnetization cycle.

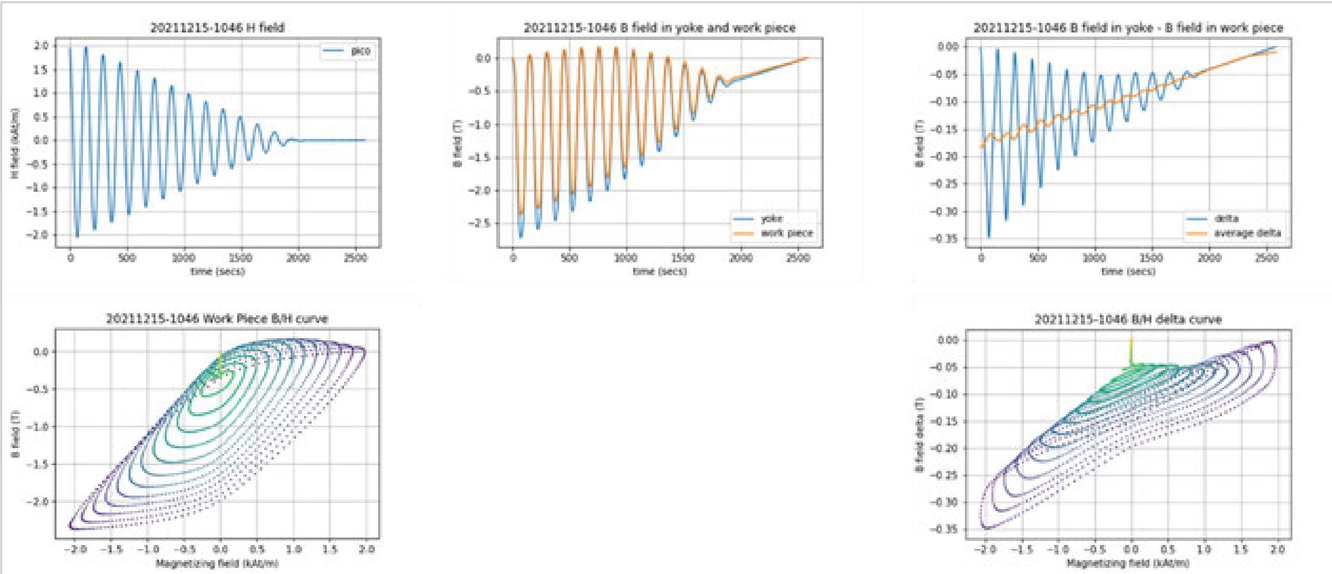

Fig. 12. Collected data from a significantly magnetized test block.

Measurement during demagnetization cycling of test blocks

The demonstrator parts came in two forms, rings and the dome lid.

The rings can be readily demagnetised if the flux is induced to go around the part. They are then, in effect, providing their own yoke for the B field and the only issue to consider is the most efficient way to wind the coils. There are suppliers of solutions for this where high current multi-pole connectors allow the coil to be clamped on – in a high current version of the search coils, see Fig. 13.

Fig. 13. Clamp-on coil for demagnetisation (photograph copyright owned by Diverse Technologies, accessed online).

The dome lids do not provide a geometry where the field is shunted within the steel and consequently an external yoke must be used to provide high enough fields to approach saturation. As the dome lids are quite large pieces, a yoke of the same form in use at TWI is suitable. The model was revised to show the yoke being applied to a dome lid, see Fig. 14.

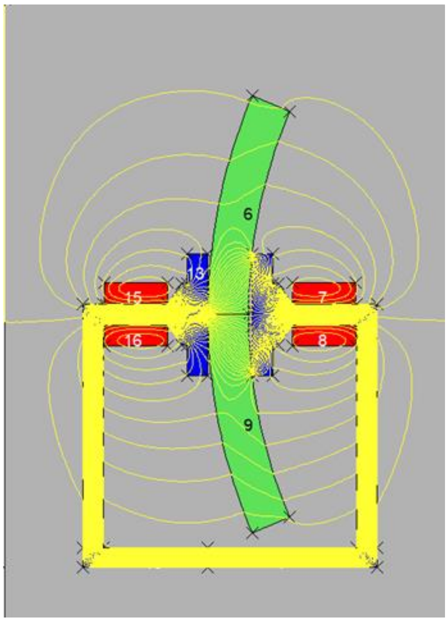

Fig. 14. Flux lines shown for demagnetization of the domed lid.

The problem with this configuration is that as soon as the domed lid between the jaws of the yoke starts to saturate, the flux will spread out wider. Consequently it will be difficult to achieve the same field without very high H fields, which will make the equipment expensive and more cumbersome to deploy.

One possible solution explored was to reduce the width of the jaws to try to concentrate the flux in a smaller area and thereby increase the B field. This approach has been modelled for a reduction of the jaw width to 300 mm and is shown in Fig. 15. Some 1T of field can be induced using this approach – which is getting close to the fields used on the test blocks.

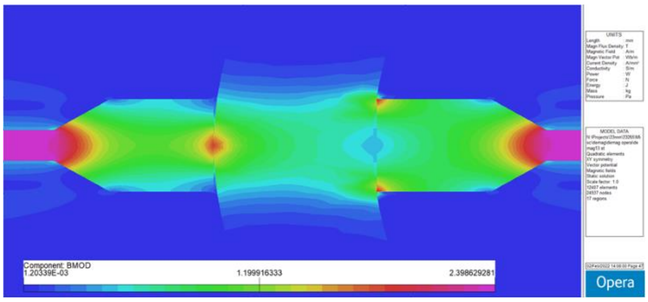

Fig. 15. Clamp-on coil for demagnetisation (photograph copyright owned by Diverse Technologies, accessed online).

The disadvantage of this approach is that the lid will require more patches of demagnetization, although these patches could be concentrated close to the weld line to give best effect in that region.

Summary

Within the reported work we have shown that modelling of TWI's demagnetization yoke for test blocks allows us to understand the *B* field magnitude in the test blocks and to ensure that we have the right combination of turns, current and magnetic path to reach a degree of saturation in the test block.

Measurement during demagnetization cycling of test blocks has allowed us to detect the *B* field and monitor this over the demagnetization cycle. Asymmetry in the detected *B* field indicates the polarisation (i.e. magnetization) of the material.

Modelling has been used to determine requirements for demagnetization of demonstrator parts, in particular the domed lid. This part presents some challenges as it is difficult to magnetically saturate it to the same level as the test blocks. However, it may be sufficient to demagnetize it with a lower *B* field induced, and this approach will be investigated in future work.

Acknowledgements

This report is on a package of work in a project led by Sheffield Forgemasters, part funded by the UK government's Department for Business, Energy & Industrial Strategy (BEIS) under the £26m Advanced Manufacturing and Materials (AMM) Programme, as part of the £505m Energy Innovation Portfolio.

Dr. Colin Ribton *- is a Technology Fellow in TWI's electron beam group in Cambridge, UK. He is a fellow of the Institute of Physics, a Chartered Physicist and a Chartered Engineer. His scientific interests include electro-magnetism, electron gun and electron optics design.*

tel.:+44 1223 899000 e-mail:colin.ribton@twi.co.uk